

Mean-field potential calculations of shock-compressed porous carbon

Y. Wang,^{1,*} Z.-K. Liu,¹ L.-Q. Chen,¹ L. Burakovsky,² D. L. Preston,² W. Luo,³ B. Johansson,^{3,4} and R. Ahuja^{3,4}

¹Materials Science and Engineering, Pennsylvania State University, State College, Pennsylvania 16802-5006, USA

²Los Alamos National Laboratory, Los Alamos, New Mexico 87545, USA

³Condensed Matter Theory Group, Department of Physics, Uppsala University, Box 530, S-751 21, Uppsala, Sweden

⁴Applied Materials Physics, Department of Materials Science and Engineering, Royal Institute of Technology, S-100 44, Stockholm, Sweden

(Received 3 September 2004; revised manuscript received 1 December 2004; published 22 February 2005)

The mean-field potential approach with first-principles total energy data as input is used to investigate shock-compressed carbon with initial densities of 3.51, 2.2, 1.85, and 1.6 g/cm³ up to 1400 GPa. We have calculated the shock Hugoniot, and the temperature and electronic contribution to the heat capacity along the Hugoniot. While excellent agreement with underground nuclear explosion data is obtained, our results do not show the high compressibility of carbon at megabar pressures indicated by recent laser-driven shock wave experiments.

DOI: 10.1103/PhysRevB.71.054110

PACS number(s): 64.10.+h, 71.15.Nc, 05.10.-a, 05.70.Ce

I. INTRODUCTION

The equation of state (EOS) of carbon has recently been investigated both experimentally and theoretically.¹⁻⁵ Very recently, Batani *et al.* carried out laser-driven shock wave studies of the EOS of porous carbon¹ and found that their measured shock Hugoniot points for two different initial densities of carbon fell below the Hugoniot derived from the SESAME tables.⁶ They pointed out that, despite the large error bars, the systematic deviation of their data from the theoretical curve indicates that the compressibility of carbon is greater than theoretical predictions, but they admit that this discrepancy may be due to systematic errors in their experimental technique. We note that EOS data on deuterium from laser-driven shock wave experiments⁷⁻¹⁰ show significant departures from the SESAME model (see Knudson *et al.*¹¹), *ab initio* calculations,¹²⁻¹⁵ and other experiments.^{11,16} While Ross and Yang¹⁷ attributed the discrepancy to the failure of the current implementation of density functional theory, Nellis¹⁸ suggested that the laser-driven shock wave results were incorrect.

If limited to the solid state, the high-pressure EOS of carbon can be reliably calculated in the quasiharmonic approximation with the phonon contribution evaluated using density functional perturbation theory.^{3,19} However, the traditional Debye-Grüneisen method^{2,20} is the most widely used approach (it is used to construct the SEASAME EOS tables) but it is not only limited to solids, but also depends on the modeled density dependence of the Grüneisen parameter (γ), such as $\gamma\rho = \text{const}$ (ρ is the density). In this paper we calculate the Hugoniot of carbon with initial densities of 3.51, 2.2, 1.85, and 1.6 g/cm³ up to 1400 GPa using the mean-field potential (MFP) approach,²¹⁻²⁶ which has been tested for many elemental materials, including porous solids.²⁷ Variations in the initial density allow us to study more of the EOS surface of carbon. (Since the MFP method incorporates the one-particle mean-field model, it is not possible to study molecular liquid deuterium without first extending the technique.)

II. THEORETICAL METHOD

We first give a brief summary of the MFP approach. In a couple of papers,^{21,22} the classical MFP approach was developed to calculate the various thermodynamic quantities of metals. The MFP approach was first tested on the metal Ce.²¹ The transition pressure and volume change of the well known γ - α isostructural transition at 300 K, the experimental Hugoniot, and the 300 K isotherm were well reproduced. The MFP approach was then checked for the five metals Al, Cu, Ta, Mo, and W.²² The calculated Hugoniot and 293 K isotherms fell well within the experimental uncertainties. The MFP yields Hugoniot for porous copper, nickel, and molybdenum in good agreement with experiment, including cases of anomalous compressibility.²⁷

Let us consider a system with a given averaged atomic volume V and temperature T . It is known that the vibrational contribution to the partition function takes the form $Z_{\text{ion}} = \exp(-NF_{\text{ion}}/k_B T)$, where N is the total number of lattice ions and F_{ion} is the vibrational free energy of an ion. In the mean-field approximation, the classical Z_{ion} is given by

$$Z_{\text{ion}} = \left(\frac{Mk_B T}{2\pi\hbar^2} \right)^{3N/2} \left\{ \int \exp[-g(\mathbf{r}, V)/k_B T] d\mathbf{r} \right\}^N. \quad (1)$$

The essential feature of the MFP approach is that the mean-field potential $g(\mathbf{r}, V)$, is simply constructed only in terms of the 0-K total energy E_c , which is obtained from *ab initio* electronic structure calculations

$$g(r, V) = \frac{1}{2} [E_c(R+r) + E_c(R-r) - 2E_c(R)]. \quad (2)$$

It has been shown²¹ that the well-known Dugdale-MacDonald²⁸ expression for the Grüneisen parameter can be derived by expanding $g(r, V)$ to order r^2 .

As a result, when the magnetic contribution is neglected, the Helmholtz free energy per ion $F(V, T)$, can be written as the sum of the cold ($T=0$), vibrational ionic, and thermal electronic contributions

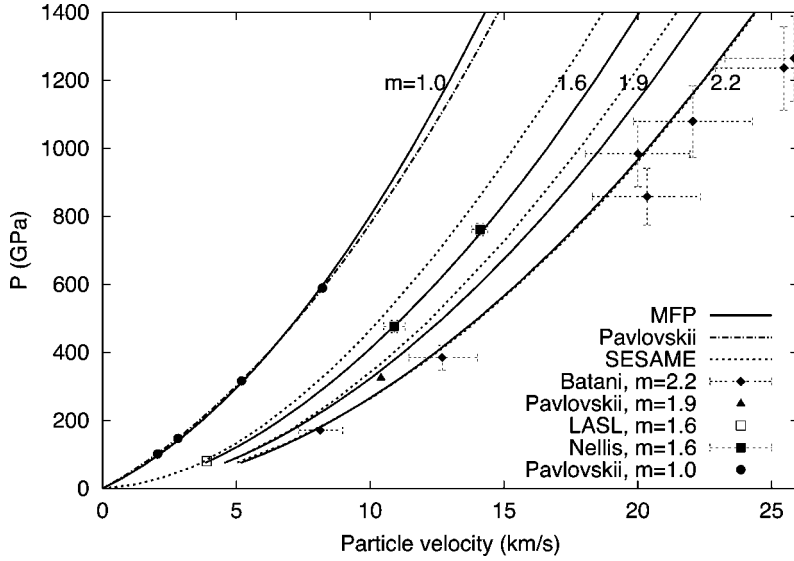


FIG. 1. Hugoniot pressure versus particle velocity of diamond for initial porosities $m=1.0$, 1.6, 1.9, and 2.2. The solid lines represent the results of the present calculation. The dot-dashed line at $m=1.0$ is the empirical fit $u_s=12.16 + 1.00u_p$ of Pavlovskii (Ref. 35); and the dotted lines at $m=1.57$ ($\rho_0=2.23$ g/cm³), $m=1.9$ ($\rho_0=1.85$ g/cm³), and 2.2 ($\rho_0=1.6$ g/cm³) were obtained by Batani *et al.* (Ref. 1) from the SESAME tables. The data points are ●: Pavlovskii (Ref. 35), □: LASL (Ref. 36), ■: Nellis (Ref. 2), ▲: Pavlovskii *et al.* (Ref. 34), and ◆: Batani *et al.* (Ref. 1).

$$F(V,T) = E_c(V) + F_{\text{ion}}(V,T) + F_{\text{el}}(V,T), \quad (3)$$

$$F_{\text{ion}}(V,T) = -k_B T \left(\frac{3}{2} \ln \frac{mk_B T}{2\pi\hbar^2} + \ln \nu_f(V,T) \right), \quad (4)$$

$$\nu_f(V,T) = 4\pi \int \exp\left(-\frac{g(r,V)}{k_B T}\right) r^2 dr, \quad (5)$$

$$F_{\text{el}} = E_{\text{el}} - TS_{\text{el}}, \quad (6)$$

$$E_{\text{el}}(V,T) = \int n(\varepsilon,V) f \varepsilon d\varepsilon - \int^{\varepsilon_F} n(\varepsilon,V) \varepsilon d\varepsilon, \quad (7)$$

$$S_{\text{el}}(V,T) = -k_B \int n(\varepsilon,V) [f \ln f + (1-f) \ln(1-f)] d\varepsilon. \quad (8)$$

In the above equations, F_{ion} is the ionic vibrational free energy, F_{el} is the free energy due to the thermal excitation of electrons, $n(\varepsilon, V)$ is the electronic density of states (DOS), f is the Fermi distribution, and ε_F is the electronic Fermi energy.

Other thermodynamic functions can be obtained in the usual way from $F(V,T)$; specifically, entropy is $S = -(\partial F / \partial T)_V$, internal energy is $E = F + TS$, pressure is $P = -(\partial F / \partial V)_T$, and the Gibbs free energy is $G = F + PV$.

III. COMPUTATIONAL DETAILS

The P - V Hugoniot was obtained from the Rankine-Hugoniot relation $P(V_0^{\text{porous}} - V)/2 = E - E_0^{\text{porous}}$, where V_0^{porous} is initial specific volume and E_0^{porous} is the initial specific internal energy. In all of our Hugoniot calculations we take the carbon structure to be that of diamond (3.51 g/cm³ ambient density); hence, our initial densities of 2.2, 1.85, and 1.6 g/cm³ correspond to ‘‘porous diamond.’’ This is a reasonable approximation since the measured enthalpy difference between diamond and graphite under standard conditions is

just -19 meV/atom (see Janotti *et al.*,²⁹ and references therein). The effect of this difference on the Hugoniot temperatures is less than 100 K, which is not discernable in the figures plotted in this paper. We only consider pressures above the graphite-diamond transformation pressure and assume the final states are completely compacted. In this case, it is a good approximation to take the initial specific energy E_0^{porous} for porous carbon to be exactly the same as the initial specific energy E_0 for nonporous carbon. The initial volume of the porous material is $V_0^{\text{porous}} = m V_0$, where m is the initial porosity and V_0 is the ambient volume of nonporous single-crystal diamond. Our initial densities of 3.51, 2.2, 1.85, and 1.6 g/cm³ correspond to $m=1.0$, 1.6, 1.9, and 2.2, respectively.

Mitchell *et al.*³⁰ found that the effects of shock melting on the P - V Hugoniot of several reference metals were too weak to be observed; hence we have neglected shock melting and the phase dependence of the high-temperature equation of state in our calculations of the carbon Hugoniot.

The 0-K total energy was calculated using the full-potential linearized augmented plane wave (LAPW) method^{31,32} in the generalized gradient approximation (GGA).³³ To ensure continuity of the calculated energy as a function of volume, we used constant muffin-tin radii of $1.0a_0$ (Bohr radius). The input to all of our thermodynamic calculations consists of both LAPW-calculated energies and points obtained by cubic spline interpolation with nodes separated by $0.005a_0$. Outside the region where the LAPW calculations are applicable, Morse function extrapolations toward zero and infinity are used to complete the 0-K energy curve.

IV. RESULTS AND DISCUSSION

A. Pressure versus particle velocity

Laser-driven shock wave data are usually presented in the u_p - P plane because of the large error bars on the measured densities. Our calculated results for $m=1.0$, 1.6, 1.9, and 2.2 are plotted in the u_p - P plane in Fig. 1 together with experi-

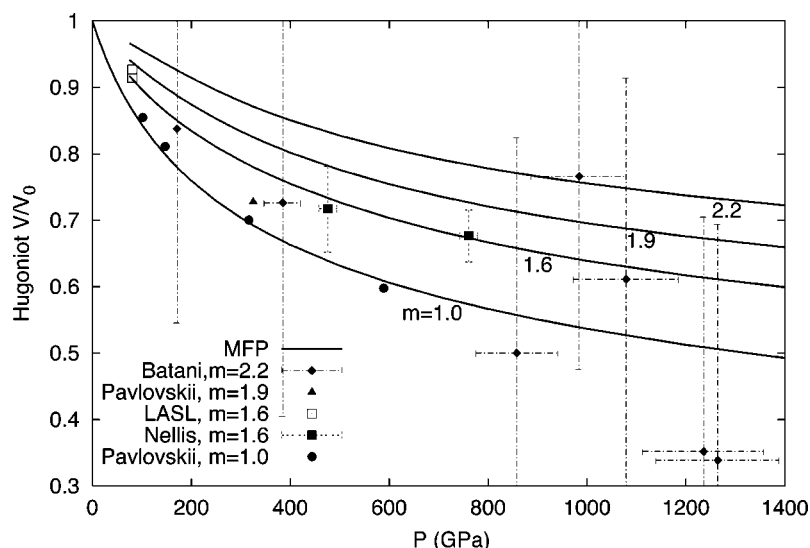


FIG. 2. Relative Hugoniot volume versus pressure for diamond with initial porosities $m = 1.0, 1.6, 1.9,$ and 2.2 . V_0 is the ambient atomic volume of single-crystal diamond. The solid lines represent the results of the present calculation. The data points are \bullet : Pavlovskii (Ref. 35), \blacktriangle : Pavlovskii *et al.* (Ref. 34), \square : LASL (Ref. 36), \blacksquare : Nellis (Ref. 2), and \blacklozenge : Batani *et al.* (Ref. 1).

mental data.^{1,2,34–36} The porosity $m=1.0$ (initial density $=3.51 \text{ g/cm}^3$) corresponds to single crystal diamond, and $m=1.6$ (initial density $=2.2 \text{ g/cm}^3$) corresponds to pyrolytic graphite. For these two porosities, our calculated u_p - P Hugoniot agree with the measurements^{2,35,36} to within the experimental error bars. For $m=1.0$, we believe that the small but growing difference between the empirical fit $u_s=12.16 + 1.00u_p$ of Pavlovskii³⁵ and our calculations above 600 GPa is a consequence of extrapolating the fit to pressures above those of the data that were available to Pavlovskii ($P < 600$ GPa). Nellis *et al.*² calculated the graphite Hugoniot by taking it to be “porous diamond” at $m=1.6$ and found that their theoretical curve deviated significantly from their measurements for $P > 300$ GPa, but still our calculations show excellent agreement with their measurements. For $m=2.2$, the laser-driven shock wave results of Batani *et al.*¹ are systematically lower than our calculations at a given particle velocity, and they are also systematically lower than the Hugoniot obtained from the SESAME tables.

Figure 1 includes the SESAME Hugoniot for $m=1.6, 1.9,$ and 2.2 obtained by Batani *et al.*¹ from the SESAME EOS of graphite ($m=1.6$). The Hugoniot for $m=1.6$ and 1.9 disagree with our MFP results, while the Hugoniot for $m=2.2$ is in close agreement. The discrepancy is most likely due to inaccuracy in the Grüneisen gamma used to construct the SESAME EOS.³⁷ The agreement between the MFP and SESAME Hugoniot for $m=2.2$ is fortuitous.

B. Relative volume (V/V_0) versus pressure

In Fig. 2, a plot of V/V_0 versus P , the errors due to the uncertainties in the particle velocity measurements are enlarged enormously. Note that the errors in the relative volume for the laser-driven shock wave experiments by Batani *et al.*¹ for $m=2.2$ span the entire volume range from $m=1.0$ to $m=2.2$ at a given pressure.

For $m=1.9$ ($\rho_0=1.85 \text{ g/cm}^3$), the relative volume measured by Pavlovskii *et al.*³⁴ at 325 GPa is 0.728. In contrast, our calculated relative volume is 0.825. The discrepancy between our calculation and the measurement by Pavlovskii

*et al.*³⁴ for $m=1.9$ may be due to inaccuracy in their measurement. We can see from Fig. 2 that the graphite Hugoniot data^{2,36} for $m=1.6$ ($\rho_0=2.2 \text{ g/cm}^3$) show a trend toward a larger value of V/V_0 than 0.728 at 325 GPa. Note that the shock experiment of Pavlovskii *et al.*³⁴ on carbon for $\rho_0=1.85 \text{ g/cm}^3$ ($m=1.9$) gives a density at 325 GPa that is higher than that obtained for $\rho_0=2.2 \text{ g/cm}^3$ ($m=1.6$) from our MFP calculations at the same pressure, or by extrapolation of the data of Nellis *et al.*² to 325 GPa.

C. Hugoniot temperatures

Our results for $m=1.0, 1.6, 1.9,$ and 2.2 are plotted in the T - V/V_0 plane in Fig. 3(a), which also shows the carbon Hugoniot temperatures for $m=1.0$ and 1.847 calculated by Pavlovskii.³⁵ Our result for $m=1.0$ is in good agreement with that of Pavlovskii, while his result for $m=1.847$ is closer to our result for $m=1.6$ than to our result for $m=1.9$. It should be mentioned that standard temperature estimates are rather uncertain due to the shortage of data on the Grüneisen parameter and specific heat.

The calculated Hugoniot temperatures as a function of pressure up to 1400 GPa are listed in Table I and compared to the model results of Fried and Howard⁴ (FH) in Fig. 3(b). At a given pressure the Hugoniot temperature increases with the porosity because of the larger volume collapse and the corresponding larger increase in internal energy. While very good agreement is obtained between our calculation and the FH modeling for $m=1.0$ (diamond) and $m=1.6$ (graphite), our calculated temperature for $m=1.9$ at 325 GPa is 21758 K, which is almost 50% higher than the 15000 K obtained by FH. FH obtained their EOS by generalizing the approximate Murnaghan functional form. The EOS parameter values were chosen to ensure agreement with two types of data: (1) accurate thermodynamic data, specifically the 300 K isotherms and temperature dependences of the heat capacities of both diamond and graphite, thus the good agreement between FH and MFP for the $m=1.0$ and $m=1.6$ Hugoniot temperatures; (2) inaccurate shock data, namely the measurement of Pavlovskii *et al.*³⁴ for $m=1.9$, which is

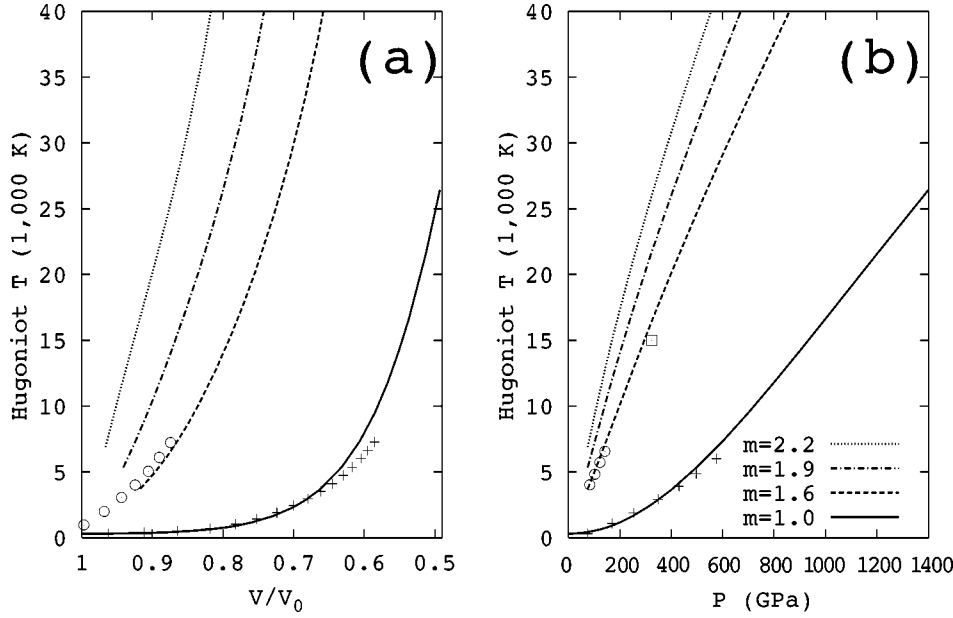


FIG. 3. Hugoniot temperatures for diamond with initial porosities $m=1.0, 1.6, 1.9,$ and 2.2 . The curves are the results of our MFP calculations. (a) Hugoniot temperature as a function of relative volume V/V_0 . The points are Pavlovskii's (Ref. 35) for $m=1.0(+)$ and $1.847(O)$, (b) Hugoniot temperature versus pressure. Here the points are from Fried and Howard (Ref. 4): $m=1.0(+)$, $1.6(O)$, and $1.9(\square)$.

inconsistent with our MFP Hugoniot (see previous subsection), hence the discrepancy between the FH and MFP Hugoniot temperatures for $m=1.9$ at 325 GPa.

D. Shock-induced insulator-conductor transition in carbon

The pressure-induced metallization of non-metals has been the subject of a number of theoretical and experimental

studies.^{38–41} At low temperatures, metallization is associated with the closing of the electronic band gap. We have calculated the electronic band gap of diamond-type carbon as a function of V/V_0 ; see Fig. 4(a). The calculated band gap increases with density, as also found by Surh *et al.*³⁹ and by Fahy and Louie.⁴⁰ This implies that diamond-type carbon becomes a more effective insulator with increasing hydrostatic pressure, in agreement with experiment.⁴¹ This unusual

TABLE I. The calculated relative volume V/V_0 and temperature for diamond with initial porosities $m=1.0, 1.6, 1.9,$ and 2.2 . V_0 is the atomic volume of single-crystal diamond under ambient conditions.

m P (GPa)	1.0		1.6		1.9		2.2	
	V/V_0	T (K)	V/V_0	T (K)	V/V_0	T (K)	V/V_0	T (K)
75	0.8726	429	0.9155	3707	0.9397	5328	0.9646	6881
100	0.8437	520	0.8952	4937	0.9242	7098	0.9538	9123
125	0.8185	637	0.8772	6201	0.9099	8875	0.9433	11307
150	0.7963	783	0.8609	7492	0.8967	10634	0.9328	13405
175	0.7768	960	0.8464	8797	0.8843	12356	0.9225	15411
200	0.7594	1165	0.8330	10106	0.8726	14032	0.9126	17333
250	0.7292	1649	0.8091	12705	0.8513	17244	0.8942	20967
300	0.7038	2229	0.7883	15244	0.8323	20288	0.8775	24387
325	0.6925	2552	0.7789	16487	0.8238	21758	0.8698	26035
350	0.6820	2897	0.7700	17711	0.8155	23197	0.8624	27649
400	0.6631	3647	0.7535	20105	0.8005	26000	0.8490	30792
500	0.6315	5367	0.7255	24708	0.7745	31366	0.8259	36823
600	0.6059	7338	0.7022	29119	0.7532	36504	0.8069	42612
700	0.5847	9507	0.6825	33389	0.7350	41481	0.7906	48230
800	0.5665	11818	0.6656	37553	0.7195	46336	0.7768	53719
900	0.5506	14215	0.6508	41633	0.7060	51094	0.7647	59106
1000	0.5366	16655	0.6379	45646	0.6944	55773	0.7540	64417
1200	0.5126	21565	0.6160	53510	0.6745	64954	0.7360	74882
1400	0.4927	26438	0.5981	61213	0.6584	73974	0.7211	85221

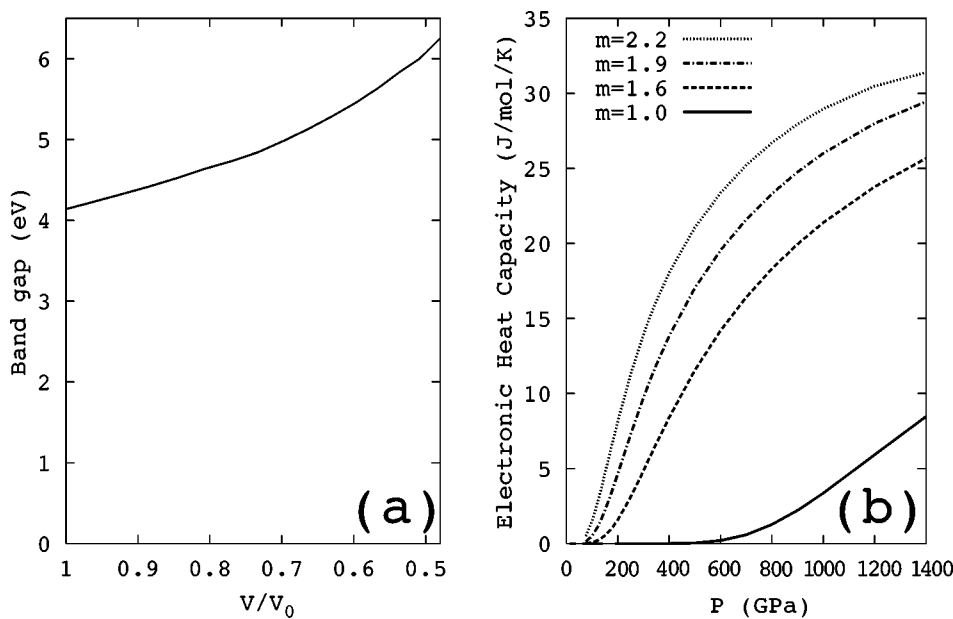


FIG. 4. (a) The calculated band gap of carbon as a function of relative volume V/V_0 . (b) The calculated electronic heat capacity of diamond as a function of pressure for initial porosities $m=1.0$, 1.6, 1.9, and 2.2.

behavior is usually explained in terms of the splitting of bonding and antibonding sp^3 states of carbon.^{39,41}

However, in the case of shock-wave compression, the increase in temperature along the Hugoniot must be taken into account, especially in the case of porous materials, which generate high temperatures during volume collapse (Fig. 3). High temperatures could excite electrons from the valence band to the conduction band of carbon, even though the band gap is very large. For $m=1.0$, 1.6, 1.9, and 2.2, we have also calculated the electronic contribution to the heat capacity $C_{el}=dE_{el}/dT$ [see Eq. (7) for the definition of E_{el}], of carbon along its Hugoniot. An abrupt increase in C_{el} from zero in the low-pressure insulating state is an unambiguous signature for the insulator-conductor transition. In Fig. 4(b), we see that while single-crystal diamond does not become a conductor until shocked up to 600 GPa, diamond with a porosity of $m=2.2$ can be transformed into a conductor by shock loading to a pressure of approximately 80 GPa.

V. SUMMARY

To summarize, the Hugoniots of carbon with porosities $m=1.0$, 1.6, 1.9, and 2.2, corresponding to initial densities of $\rho_0=3.51$, 2.2, 1.85, and 1.6 g/cm³, respectively, have been calculated by the MFP approach. The present calculation shows excellent agreement with the underground nuclear ex-

plosion data^{2,35} at $m=1.0$ (single-crystal diamond) and 1.6 (graphite). In contrast, our calculations do not show the high compressibility of carbon at megabar pressures observed by Batani *et al.*¹ in their very recent laser-driven shock wave experiment, nor do our MFP results support the measurement of Pavlovskii *et al.*³⁴ for $m=1.9$. In addition, we also studied the possible insulator-metal transition in shocked carbon. We found that single-crystal diamond will not transform into a metal until shocked up to 600 GPa, but porous diamond with $m=2.2$ is predicted to transform into a metallic state at $P=80$ GPa.

ACKNOWLEDGMENT

This work was supported by the National Science Foundation through Grants No. DMR-9983532 and DMR-0122638. Calculations were carried out on the IBM-SP3 supported by the DOD High Performance Computer Modernization Program at the ASC-MSRC and the LION-XL cluster at Pennsylvania State University supported in part by NSF Grant No. DMR-0205232 and in part by the Materials Simulation Center led by Dr. Sofo at Pennsylvania State University. This work was also supported in part by the Swedish Foundation for Strategic Research (SSF), the Swedish Natural Science Research Council (NFR), and the Göran Gustafsson Foundation. Two of us (L.B., D.L.P.) wish to thank J.D. Johnson for very valuable discussions on the equation of state of carbon.

*E-mail address: yuw3@psu.edu

¹D. Batani, F. Strati, H. Stabile, M. Tomasini, G. Lucchini, A. Ravasio, M. Koenig, A. Benuzzi-Mounaix, H. Nishimura, Y. Ochi, J. Ullschmied, J. Skala, B. Kralikova, M. Pfeifer, C. Kadlec, T. Mocek, A. Prag, T. Hall, P. Milani, E. Barborini, and P. Piseri, Phys. Rev. Lett. **92**, 065503 (2004).

²W. J. Nellis, A. C. Mitchell, and A. K. McMahan, J. Appl. Phys.

90, 696 (2001).

³K. Kunc, I. Loa, and K. Syassen, Phys. Rev. B **68**, 094107 (2003).

⁴L. E. Fried and W. M. Howard, Phys. Rev. B **61**, 8734 (2000).

⁵L. M. Ghiringhelli, J. H. Los, E. J. Meijer, A. Fasolino, and D. Frenkel, Phys. Rev. B **69**, 100101 (2004).

⁶T4 Group, LANL, Los Alamos, 1983.

- ⁷L. B. DaSilva, P. Celliers, G. W. Collins, K. S. Budil, N. C. Holmes, T. W. Barbee, B. A. Hammel, J. D. Kilkenny, R. J. Wallace, M. Ross, R. Cauble, A. Ng, and G. Chiu, *Phys. Rev. Lett.* **78**, 483 (1997).
- ⁸G. W. Collins, L. B. Da Silva, P. Celliers, D. M. Gold, M. E. Foord, R. J. Wallace, A. Ng, S. V. Weber, K. S. Budil, and R. Cauble, *Science* **281**, 1178 (1998).
- ⁹Y. M. Gupta and S. M. Sharma, *Science* **277**, 909 (1997).
- ¹⁰A. N. Mostovych, Y. Chan, T. Lehecha, A. Schmitt, and J. D. Sethian, *Phys. Rev. Lett.* **85**, 3870 (2000).
- ¹¹M. D. Knudson, D. L. Hanson, J. E. Bailey, C. A. Hall, and J. R. Asay, *Phys. Rev. Lett.* **90**, 035505 (2003).
- ¹²S. A. Bonev, B. Militzer, and G. Galli, *Phys. Rev. B* **69**, 014101 (2004).
- ¹³B. Militzer, D. M. Ceperley, J. D. Kress, J. D. Johnson, L. A. Collins, and S. Mazevet, *Phys. Rev. Lett.* **87**, 275502 (2001).
- ¹⁴M. P. Desjarlais, *Phys. Rev. B* **68**, 064204 (2003).
- ¹⁵B. Militzer and D. M. Ceperley, *Phys. Rev. Lett.* **85**, 1890 (2000).
- ¹⁶M. D. Knudson, D. L. Hanson, J. E. Bailey, C. A. Hall, J. R. Asay, and W. W. Anderson, *Phys. Rev. Lett.* **87**, 225501 (2001).
- ¹⁷M. Ross and L. H. Yang, *Phys. Rev. B* **64**, 174102 (2001).
- ¹⁸W. J. Nellis, *Phys. Rev. Lett.* **89**, 165502 (2002).
- ¹⁹J. J. Xie, S. P. Chen, J. S. Tse, S. de Gironcoli, and S. Baroni, *Phys. Rev. B* **60**, 9444 (1999).
- ²⁰B. K. Godwal, R. S. Rao, A. K. Verma, M. Shukla, H. C. Pant, and S. K. Sikka, *Laser Part. Beams* **21**, 523 (2003).
- ²¹Y. Wang, *Phys. Rev. B* **61**, R11 863 (2000).
- ²²Y. Wang, D. Chen, and X. Zhang, *Phys. Rev. Lett.* **84**, 3220 (2000).
- ²³L. Li and Y. Wang, *Phys. Rev. B* **63**, 245108 (2001).
- ²⁴Y. Wang and Y. F. Sun, *Chin. Phys. Lett.* **18**, 864 (2001).
- ²⁵Y. Wang, R. Ahuja, and B. Johansson, *J. Phys.: Condens. Matter* **14**, 10895 (2002).
- ²⁶Y. Wang, R. Ahuja, and B. Johansson, *High Press. Res.* **22**, 485 (2002).
- ²⁷Y. Wang, R. Ahuja, and B. Johansson, in *Shock Compression of Condensed Matter-2001*, edited by M. D. Furnish, N. N. Thadhani, and Y. Horie, AIP Conf. Proc. No. 620 (American Institute of Physics, Melville, 2002), p. 67.
- ²⁸J. S. Dugdale and D. K. C. MacDonald, *Phys. Rev.* **89**, 832 (1953).
- ²⁹A. Janotti, S. H. Wei, and D. J. Singh, *Phys. Rev. B* **64**, 174107 (2001).
- ³⁰A. C. Mitchell, W. J. Nellis, J. A. Moriarty, R. A. Heinle, N. C. Holmes, R. E. Tipton, and G. W. Repp, *J. Appl. Phys.* **69**, 2981 (1991).
- ³¹P. Blaha, K. Schwarz, G. Madsen, D. Kvasnicka, and J. Luitz, WIEN2K, <http://www.wien2k.at/>
- ³²P. Blaha, K. Schwarz, and J. Luitz, Improved and updated Unix version of the original copyrighted WIEN code, which was published by P. Blaha, K. Schwartz, P. Sorantin, and S. B. Trickey, *Comput. Phys. Commun.* **59**, 399 (1990).
- ³³J. P. Perdew, K. Burke, and M. Ernzerhof, *Phys. Rev. Lett.* **77**, 3865 (1996).
- ³⁴M. N. Pavlovskii and V. P. Drakin, *Sov. Phys. Solid State* **4**, 116 (1966).
- ³⁵M. N. Pavlovskii, *Sov. Phys. Solid State* **13**, 741 (1971).
- ³⁶*LASL Shock Hugoniot Data*, edited by S. P. Marsh (University of California Press, Berkeley, 1980).
- ³⁷J. D. Johnson (private communication).
- ³⁸A. K. McMahan, *Physica B & C* **139 & 140**, 31 (1986).
- ³⁹M. P. Surh, S. G. Louie, and M. L. Cohen, *Phys. Rev. B* **45**, 8239 (1992).
- ⁴⁰S. Fahy and S. G. Louie, *Phys. Rev. B* **36**, 3373 (1987).
- ⁴¹*Landolt-Bornstein Tables*, edited by O. Madelung, M. Schulz, and H. Weiss (Springer, Berlin, 1982), Vol. 17a.